Impact of Gas Flaring on Air Quality and Public Health in Southeastern City of Unyenge-Mbo, Nigeria

Tyoyima John Ayua [1,*], Idongesit Sunday Ambrose [2], Unyime Ukoette Saturday [3], and Silas Ijah Ioryue [4]

[1] Division of Physical and Natural Sciences, School of Arts and Sciences, University of the Gambia, Serekunda, The Gambia
[2] Department of Microbiology, Federal University of Technology, Ikot Abasi, Nigeria
[3] Department of Geography and Natural Resources Management, University of Uyo, Uyo, Nigeria
[4] Department of Biochemistry, Federal University of Technology, Ikot Abasi, Nigeria
Email: tayua@utg.edu.gm (T.J.A.); adonambrose@futia.edu.ng (I.S.A.); unyimesaturday2002@yahoo.com (U.U.S.); silasoo4real@gmail.com (S.I.I.)
*Corresponding author
Manuscript received January 16, 2026; revised March 15, 2026; accepted April 9, 2026; published August 24, 2026

Abstract*—Gas flaring from stacks in the Niger Delta region of Nigeria emits hazardous pollutants that degrade air quality and pose health challenges. Seasonal weather patterns, Harmattan winds, and rainfall further influence pollutant dispersion and community exposure. This study presents the spatiotemporal distribution of gas-flare emitted pollutants from the stack and their relationship with meteorological factors from 2023 to 2025 using an Altair 5X multi-gas detector and an Air Ae Steward Air Quality Monitor. ARC-GIS Version 10.8 dispersion modeling and Environmental Protection Agency (EPA-454/B-24-002)-based Air Quality Index (AQI) calculations were performed to evaluate the spatial patterns of the pollutants, and Analysis of Variance (ANOVA) was used to assess seasonal changes. One-way ANOVA revealed significant seasonal variation for all pollutants ($p < 0.001$). The strongest seasonal effects were observed for $PM_{2.5}$ ($F(3,32) = 18.2$, $\eta^2 = 0.63$), PM_{10} ($F = 16.4$, $\eta^2 = 0.60$), and CO ($F = 14.6$, $\eta^2 = 0.58$), indicating that season explained 49–63% of total concentration variability. NO_2 ($F = 12.8$, $\eta^2 = 0.52$) and SO_2 ($F = 11.5$, $\eta^2 = 0.49$) also showed large seasonal effects. Post-hoc analysis confirmed significantly higher concentrations during the dry/Harmattan season (Q1). Distance-based Analysis of Variance (ANOVA) demonstrated significant radial decay for all pollutants ($p \leq 0.004$), with moderate to large effect sizes ($\eta^2 = 0.29$–0.39). Seasonal influence consistently exceeded spatial effects, highlighting the dominant role of atmospheric stability in pollutant accumulation. Particulate matter exhibited the greatest seasonal amplification, indicating elevated exposure risk during dry-season conditions. These findings emphasize the need for seasonally targeted emission control and monitoring strategies in gas flare-impacted communities to reduce exposure and protect vulnerable populations in flare-affected areas.

***Keywords*—gas flaring, air quality, criteria pollutants, meteorological factors, pollutants dispersion, public health**

I. Introduction

Gas flaring from nearby oil and gas operations releases a toxic cocktail of pollutants that severely degrades local air quality [1]. The Unyenge community, located in Mbo Local Government Area of Akwa Ibom State within Nigeria's Niger Delta region, has endured severe environmental degradation and chronic air pollution largely stemming from intensive oil and natural gas extraction activities [1, 2], resulting in a wide array of interconnected adverse impacts that have profoundly affected both the ecosystem and local livelihoods.

These operations have contributed to sharply reduced agricultural productivity, with noticeable declines in cassava (staple food) yields as well as impaired flowering and fruiting in economically vital palm trees, while residents have reported increased incidences of serious health problems, including childhood malformations, liver damage, various skin conditions, and other pollution-linked illnesses. At the same time, airborne pollutant concentrations have risen significantly, leading to acidification of soils and rainwater, accelerated corrosion of metal roofing materials commonly used in homes, and elevated levels of sulfate, nitrate, and total dissolved solids in environmental media, all of which compound the ecological damage and further disrupt farming and water quality. These physical and chemical changes have, in turn, triggered broader socioeconomic challenges, such as diminished household incomes, food insecurity, community hardship, and strained social structures, illustrating the multifaceted and cascading consequences that oil and gas activities continue to impose on host communities in the Niger Delta [2, 3].

Gas flaring—the routine combustion of associated natural gas during oil extraction—has endured for more than 160 years, driven by persistent economic, infrastructural, and regulatory barriers that prevent its capture, utilization, or reinjection [4, 5]. In 2024, global flaring volumes reached approximately 151 billion cubic meters (bcm), marking the highest level since 2007 and a slight increase from 148 bcm in 2023, according to the World Bank's Global Gas Flaring Tracker. This wasteful practice released an estimated 389 million tons of CO_2 equivalent (CO_2e) emissions, including about 46 million tonnes from unburnt methane—a potent greenhouse gas—surpassing the total annual emissions of entire countries like Egypt (based on 2023 figures) and contributing significantly to global climate change. Inefficient flare combustion not only emits substantial CO_2 but also allows methane slippage, adding roughly 46 million tonnes of CO_2e from incomplete burning alone, while the overall inefficiency exacerbates the climate impact beyond direct CO_2 releases.

Beyond its environmental toll, flaring squanders a valuable energy resource that could otherwise fuel power generation, industrial processes, or domestic use, thereby undermining energy security, access in developing regions, and broader efforts to mitigate greenhouse gas emissions. Gas flaring is a common practice to safely dispose of excess gas when it is not economically feasible or practical to capture and transport. It is the controlled burning of natural gas that is produced as a byproduct of oil extraction. Because it releases greenhouse gases and air pollutants, it is regarded as a

wasteful and polluting technique, even though it is a safer option than releasing raw gas [6, 7]. Gas flaring is a significant contributor to the emission of criteria pollutants, such as NO_2, SO_2, CO, $PM_{2.5}$, and PM_{10}, which cause low air quality and health hazards to people because of their immediate dissemination once released into the air [2, 6–11]. According to GGFTR [5], most of the gas flared globally is produced in association with crude oil (associated gas). Flaring intensity is the volume of gas flared, in cubic meters, per barrel of oil produced. The wet and dry climates in the Niger Delta include a tropical wet pineapple climate from April to October and a tropical monsoon climate from November to March, which influences pollutant dispersion through variations in meteorological factors such as temperature, relative humidity, wind speed, and wind direction [12].

Johnson *et al.* [13] outlined 3 primary types of flaring that exist in the oil and gas industry: (i) Production flaring, which can continue for years while oil is being produced. (ii) Process flaring, which can occur at a downstream plant during a planned process blowdown in the upstream industry during well test flaring to determine the size of a reservoir. These releases can be large or small and last for a few minutes, hours, or days. (iii) Emergency flaring: this is a large, unplanned, and very short-duration release, usually at larger downstream facilities or offshore platforms. Transmission pipes, whereas heavy oil wells and upstream production locations handle the majority of the venting. Individual sources of vented gas are typically small, despite the fact that combined amounts are typically rather large [3].

Adequate knowledge of the indicators of the dispersion process from flare stacks is essential for risk exposure management and health impact assessments [14]. For example, NO_2 and SO_2 diminish exponentially because of dilution and wind effects beyond 200 m according to Ologunorisa [1]. Despite internal efforts to reduce flaring and venting, not much has been achieved. Although individual countries have had varied degrees of success, such as the Province of Alberta and Canada, where flared and vented quantities have decreased by 51% [15].

Many scientists have researched gas flaring because of its numerous hazards to human health and ecology, yet the problem persists today [3, 16].

Fawole *et al.* [17] utilized ARC-GIS Version 10.8 modeling to reveal that PM_{10} and SO_2 surpassed the World Health Organization (WHO) thresholds at 100 m, particularly under stable atmospheric conditions. Ehumadu *et al.* [18] and Akpoyibo and Vwavware [19] recorded $PM_{2.5}$ levels of 20 μg/m³ at 100 m in Delta State; however, they did not consider seasonal effects. Seasonal effects and meteorological variables have a critical effect on pollutant dispersal, and hence, on health. For instance, as Nwosisi *et al.* [20] observed, the slowing of wind speeds in the Harmattan season boosts pollutant concentrations around the flare stack, whereas in the wet season, wind helps disperse it quickly. Similarly, the highly moist 70–90% rainy season increases $PM_{2.5}$ and PM_{10} concentrations via particle aggregation, whereas the dry Harmattan season enhances particulate levels through reduced wet deposition [21]. These findings demonstrate the need to include meteorological factors when assessing air quality.

Despite extensive research on gas flaring and air quality in the Niger Delta, important knowledge gaps remain. Most previous studies have relied on annual averages or regional-scale data, with limited attention to seasonal variability and distance-specific pollutant behavior near flare stacks. In particular, very few investigations have provided simultaneous measurements of multiple criteria pollutants (NO_2, SO_2, CO, $PM_{2.5}$, and PM_{10}) at defined radial distances from active flare sites. Existing studies also tend to examine either pollutant levels or meteorological influences, but rarely integrate high-resolution field measurements with meteorological parameters and spatial modeling. Furthermore, the use of advanced portable multi-gas monitoring devices remains uncommon in Niger Delta research due to technical and financial constraints, resulting in limited real-time exposure data for vulnerable host communities.

This study addresses these gaps by providing seasonal, distance-resolved air quality measurements (60 m, 200 m, and 500 m from the flare stack) over a 3-year period (2023–2025) in Unyenge, supported by meteorological analysis and ArcMap-based spatial modeling. By combining field monitoring with spatial and seasonal analysis, this research offers improved exposure characterization for flare-impacted communities. The findings are significant because they generate location-specific and season-specific evidence needed for public health risk assessment, environmental justice advocacy, and targeted air quality management policies in the Niger Delta.

Gas flaring has a disproportionate impact on marginalized communities, emphasizing environmental justice and public health, similar to industrial chemicals, as reported by Thompson *et al.* [22]. Nriagu *et al.* [23] found that $PM_{2.5}$ and SO_2 levels were associated with flaring-related increases in asthma and bronchitis occurrences. Elijah [24] further stresses this issue, focusing on the socio-economic burden in flaring-exposed rural areas such as Unyenge, "where they have no access to large-scale monitoring and mitigation technologies, increasing the burden of disease". While these studies touch upon health and equity, their main limitation is the lack of specific data on the pollutant's concentration at certain distances. Our new method will assist in addressing these limitations by providing data on seasonal variability in pollutant levels at specified locations.

Similarly, Nriagu *et al.* [23] and Esavwede and Oyibodoro [25] reported that flaring raises $PM_{2.5}$, SO_2, and NO_2 levels above the World Health Organization (WHO), guidelines ($PM_{2.5}$: 5 μg/m³ annual mean; SO_2: 40 μg/m³ 24 h mean; NO_2: 10 μg/m³ annual mean), with consequent increases in respiratory and cardiovascular morbidity. Yakubu [26] stated that CO and particulate matter have maximum concentrations within 100 m and a later decline in concentrations at 500 m due to air dilution. While the majority of the aforementioned studies have focused on the air quality impact of flaring, few have presented seasonal data at varying distances. For instance, Nriagu *et al.* [23], Yakubu [26] contain such data; however, they present annual or district-level measurements in general rather than seasonal results at 60, 200, and 500 m from the flare stack. Nwosisi *et al.* [20] noted the influence of meteorological factors on pollutant dispersion; however, no studies have combined

these with high-resolution pollutant data; hence, more studies are needed in this area.

Finally, there is an issue of employing advanced portable tools, such as the Altair 5X multi-gas detector, which is rare in Niger Delta studies owing to technical and financial factors. This is another measurement gap that this research aims to fill in Unyenge. This study seeks to address the identified gaps by conducting NO_2, SO_2, CO, $PM_{2.5}$, and PM_{10} seasonal measurements at distances allocated within Unyenge, supported by ARCMAP modeling, and meteorological parameters (temperature, relative humidity, wind speed, and wind direction) and public health data.

To achieve this, data for 3 years (2023 to 2025) were collected using an Altair 5X multi-gas detector and Air Ae Steward Air Quality Monitor to facilitate community awareness of the gas flaring impact. It is hoped that these findings will be used to advocate for environmental justice policies and enable action in the form of air quality management, public health initiatives, and continued monitoring of the Niger Delta gas flare areas.

The structure of the paper is designed such that Section II presents the study area, dataset description, and analytical procedures used, Section III presents the results and discussions, and Section IV provides a detailed summary and conclusion of the findings.

II. Materials and Methods

A. The Study Area and Justification of Measurement Tools and Procedures

Unyenge is located between latitudes 4. 32° and 5.33°N and longitudes 7.25° and 8.25°E in the Mbo LGA of Akwa Ibom State, Nigeria [27]. It is surrounded by the Atlantic Ocean and Cameroon to the south; Urue-Offong/Oruko LGA to the north; Udung Uko Local Government Area (LGA) to the east; and Esit Eket and Ibeno LGAs to the west. The dominants inhabitants of Unyenge are the Oron ethnic group, speaking the Oro language, followed by the Efik people and other minority dialects; it is culturally homogeneous to the broader Oron nation of the Niger Delta [2]. The central study location is predominantly agrarian, with fishing as the main occupation of the people. The southern boundary alongside the Atlantic Ocean serves the people well in their quest for seafood, mainly catfish and shrimp. The presence of Universal Energy Resources Limited (UERL), Operating Oil Mining Lease (OML) 14 since 2012, demonstrates the importance of oil and gas in the area; however, gas flaring frequently occurs in the area, as shown in Fig. 1, thereby presenting significant air quality and potential health problems, particularly respiratory issues.

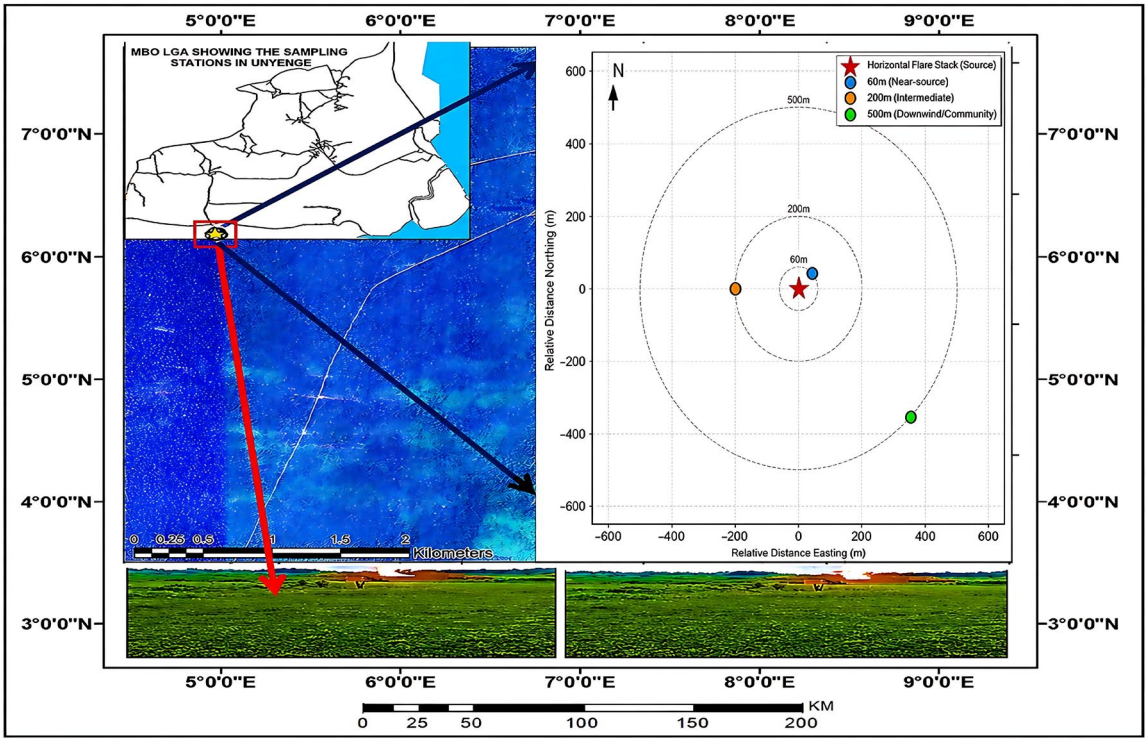

Fig. 1. Map of the study area showing sampling points and horizontal flare stacks.

As shown in Fig. 1, the flare stacks sparked community protests against United Exploration Rivers Limited (UERL) in 2013 and 2023, with highlighted demands for local jobs and social development. Unyenge continues to face environmental injustice and challenges owing to pollution and limited infrastructure. Its coastal ecosystem, part of Akwa Ibom's 129 km coastline, is threatened by oil activities. Socially, the community resisted boundary changes in 2023 and condemned a militant attack on UERL workers in 2022, advocating for peace. Despite the proposed 13.6 km road project in 2022, development lags. Unyenge's leadership continues to push for environmental protection and equitable resource allocations.

This background motivated the study and researchers to use a highly sensitive, well-calibrated Altair 5X multi-gas detector and Air Ae Steward Air Quality Monitor, among others, as shown in Table 1, to measure the pollutant concentrations and meteorological parameters quarterly at 60 m, 200 m, and 500 m, as shown in Fig. 1, from the flare stack to assess the health risk and provide useful comparative insights for continued observation of gas flaring areas.

Table 1. Spatial and temporal sampling protocols for the gas flare emission assessment

S/N	Parameter	Details	S/N	Parameter	Details
1	Study pollutants	CO, NO_2, SO_2, PM_{10} and $PM_{2.5}$	6	Sampling window	Periods of peak flaring activity (confirmed visually)
2	Spatial design	Radial transects (Downwind, Upwind, Crosswind)	7	Stabilization period	20 min per station
3	Distance zones	Zone 1 (<60 m), Zone 2 (60 m–200 m), Zone 3 (>500 m)	8	Reading duration	10-min average per reading
4	Total sampling stations	(6 Downwind, 2 Upwind, 2 Crosswind) $N = 10$	9	Replication strategy	Recorded in triplicate at each point ($n = 3$)
5	Sampling height	1.5 m (Handheld; Breathing Zone)	10	Temporal frequency	Wet Season: Monthly; Dry Season: Bi-monthly

The Altair 5X multi-gas detector was selected for this study to measure the gaseous pollutants due to its robust electrochemical sensors, which are specifically designed for high-concentration industrial environments. Its suitability for near-source flare monitoring is further supported by its real-time response capability, built-in alarm threshold validation, and detection ranges tailored to industrial emissions. While the device is not a fixed regulatory station, it is a standard tool in occupational safety and industrial monitoring for characterizing high-level gas exposure rather than determining regional regulatory compliance, and is suitable for the aim of this study. While particulate matter ($PM_{2.5}$ and PM_{10}) was measured using the Air Ae Steward monitor, which was selected for its laser scattering technology and its ability to provide real-time mass concentration outputs. The device offers a detection range of up to 500 μg/m^3 for $PM_{2.5}$, making it a practical screening-level tool for assessing environmental exposure; however, it was utilized specifically for this purpose rather than as a regulatory reference-grade monitor.

B. Study Design and Sampling Framework

To assess pollutant concentration gradients effectively, we carried out a repeated seasonal field-monitoring design around an active horizontal gas flare stack in Unyenge, Mbo LGA, Nigeria. Monitoring was conducted quarterly from January 2023 to June 2025, covering 4 distinct periods: the dry season (January–March), early wet season (April–June), peak wet season (July–September), and the late wet/transitional phase (October–December). Sampling took place at 3 fixed radial distances of 60 m, 200 m, and 500 m to represent near-source, intermediate, and downwind community exposure zones, effectively capturing plume decay gradients and potential human impact as shown in Fig. 2.

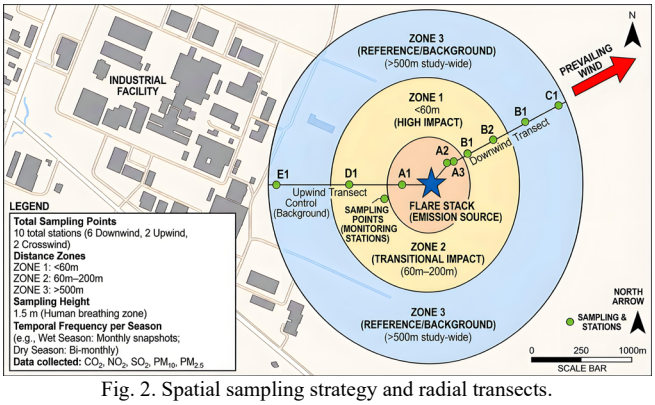

Fig. 2. Spatial sampling strategy and radial transects.

As shown in Fig. 2, at each specified distance, the measuring instruments were handheld at 1.5 m above ground level to reflect average human breathing height. To ensure data accuracy, each parameter was recorded in triplicate during periods of peak flaring activity, which were confirmed through visual observation. The sampling protocol for each point included a 20 min stabilization period followed by an averaged 10 min reading to determine the pollutant concentration for that specific zone, as shown in Table 1.

C. Instrumentation, Calibration, and Measurement Uncertainty

All monitoring instruments (Altair 5X multi-gas detector and Air Ae Steward Air Quality Monitor) were calibrated according to manufacturer specifications prior to deployment, and routine zero and span checks were performed during field measurements to reduce sensor drift and cross-sensitivity.

The Altair 5X multi-gas detector technical specifications ensure precise monitoring of key pollutants, featuring detection limits of 0–50 ppm for NO_2, 0–200 ppm for SO_2, and 0–1999 ppm for CO. Its resolution is 0.1 ppm for (NO_2/SO_2) and 1ppm for CO. Mine Safety Appliances (MSA) [28] pointed its robust sensor technology provides a manufacturer-stated accuracy of ±3% of the full scale for its electrochemical sensors. This high level of resolution and stability makes the Altair 5X an appropriate choice for capturing the significant pollutant gradients found in proximal flaring zones.

The distance of 60 m, 200 m, and 500 m were identified as hot spot locations that were mostly affected by gas flaring and were selected for monitoring. The choice of distances of 60 m, 200 m, and 500 m from the flare stack were selected to assess how pollutant concentrations change with increasing distance from the point source, representing near-source, intermediate, and farther exposure zones. This design allows evaluation of pollutant dilution and dispersion patterns, while accounting for the influence of meteorological factors such as temperature, relative humidity, wind speed, and wind direction on concentration variability. Data collection was complemented by dispersion modeling (ARC-GIS Version 10.8) to analyze spatial and temporal variations in pollutant levels, with comparisons against the World Health Organization (WHO) and Federal Ministry of Environment (FMEnv) guidelines to provide insights into the human health toxicity potential that may exist.

To ensure data integrity prior to measurements, several rigorous quality control procedures were implemented, starting with the verification of factory calibration before field deployment. During the study, zero calibration was conducted daily in clean air, while span calibration was performed using certified calibration gas cylinders prior to

each quarterly campaign. Additionally, bump tests were carried out before daily sampling to confirm sensor responsiveness, and drift correction was verified against span gas post-measurement to maintain consistency across all data points including detailed calibration of instrument as in the following sections.

D. Altair 5X Multi-Gas Detector Calibration

As shown in Fig. 3, the compact Altair 5X multi-gas detector can monitor up to five gases simultaneously.

Fig. 3. Altair 5X multi-gas detector.

Before sampling, the Altair 5X multi-gas detector was calibrated by a specialist to ensure measurement accuracy. Each sensor was supplied with a demand flow regulator and a calibration gas cylinder of known concentrations. The procedure was as follows:

i. Activation: The device was powered on by holding the center button for 5 s. The initial fresh air setup prompt was bypassed.
ii. Mode Selection: Calibration mode was accessed by holding the right button until the "press the button for zero calibration" prompt appeared.
iii. Zero Calibration: A zero calibration was performed in a clean air environment by pressing the left button, establishing an accurate baseline.
iv. Span Calibration: A demand flow regulator was attached to the calibration gas cylinder and connected to the monitor's inlet port via tubing. The process was initiated by pressing the left button when prompted.
v. Verification: Monitor readings were monitored during the process to ensure they aligned with the certified gas concentrations listed on the cylinder.
vi. Completion: Once the sensors adjusted to the correct values, the tubing was disconnected. The device then automatically returned to its standard operating mode.
vii. Bump Testing: Finally, bump tests were conducted to verify the Altair 5X multi-gas detector's functionality prior to daily deployment.

E. Calibration of Air Ae Steward Air Quality Monitor

As shown in Fig. 4, the Air Ae Steward Air Quality Monitor is a multi-functional air quality monitor that provides real-time data to assist users in creating a healthy home environment by tracking and measuring indoor air pollutants such as formaldehyde, Total Volatile Organic Compounds (TVOC), and Particulate Matter (PM). It has a resolution of 1.0 μg/ m^3 and detection limits of 0–500 μg/ m^3 for $PM_{2.5}$ and 0–999 μg/m^3 for PM_{10}. Its precision is reported typically within 1 μg/m^3 for concentrations less than 50 μg/ m^3 based on the findings of Ayua *et al.* [29].

The Air Ae Steward Air Quality Monitor features a digital display that provides real-time temperature, humidity, and pollutant measurements to support informed decision-making. While the unit requires a standard "zero-point" calibration in clean air, particularly for Volatile Organic Compounds (VOC), formaldehyde, and $PM_{2.5}$ sensors—a comprehensive multi-point calibration was performed using the following protocol:

i. Environmental Preparation: The device was placed in a well-ventilated area shielded from direct sunlight and localized pollution sources, such as smoke, cooking fumes, strong odors, or Heating, Ventilation and Air Conditioning (HVAC) vents, to ensure a stable clean-air baseline.
ii. Power Management: The unit was fully charged prior to activation.
iii. Conditioning: Following activation, the device remained in a fixed location for a 24 h automatic calibration period to acclimate to the environment.
iv. Monitoring: The interface was monitored to ensure readings remained active; consecutive 0.000 values were flagged to determine if further configuration was necessary.
v. Stabilization: The device was allowed to stabilize completely before sampling commenced, with all resulting data displayed on the integrated screen.

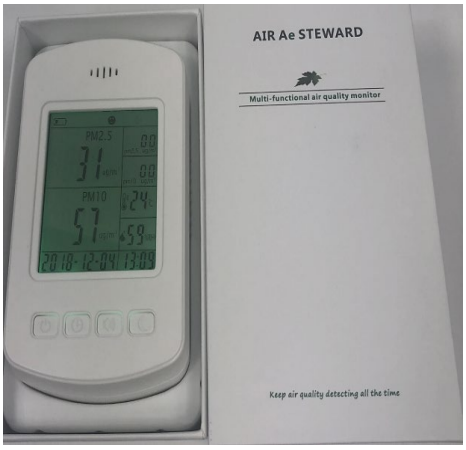

Fig. 4. Air ae steward air quality monitor.

In addition to the calibration procedures described above, measurement reliability was further strengthened by collecting triplicate measurements at each location and using boxplot analysis for outlier screening. The final measurement uncertainty was estimated by combining repeated sampling variability with manufacturer-stated accuracy, resulting in an approximate combined uncertainty of ±5–8% for gaseous pollutants and ±10% for particulate matter. These steps collectively ensured that the instrumentation in Table 2 provides a robust characterization of the local atmosphere as reported by Ayua *et al.* [29].

Table 2. Gaseous emissions and meteorological measuring instruments [30]

Parameter	Equipment	Detection Limits	Alarm Levels
Sulphur dioxide (SO_2) (ppm)	Altair 5X multi-gas detector P/N: 767951K	0–200 ppm	2.0 ppm
Nitrogen dioxide (NO_2) (ppm)	Altair 5X multi-gas detector P/N: 767951K	0–50 ppm	3.0 ppm
Carbon monoxide (CO) (ppm)	Altair 5X multi-gas detector P/N: 767951K	0–1999 ppm	35 ppm
$PM_{2.5}$, PM_{10}, (μg/m^3)	Air Ae Steward Air Quality Monitor	$PM_{2.5}$ = 0–500 μg/m^3 PM_{10} = 0–999 μg/m^3	-
Relative Humidity (%), Temperature (°C)	Max-Min Thermometer, Hygrometer Model: KTJ TA318	25–98% 0–50 °C	-
Wind speed (m/s)	MASTECH MS6252A DigitalAnemometer	0–35 m/s	-
Wind direction, Atmospheric Pressure (hPa)	Sun Road Digital compass (Altimeter) Model: CR2032	-	-

F. Dispersion Modeling Approach

Dispersion analysis was carried out using ArcGIS Version 10.8 to model the spatial distribution of air pollutants around the flare stack. Measured concentrations of NO_2, SO_2, CO, $PM_{2.5}$, and PM_{10} collected at defined sampling distances were incorporated into the Geographic Information System (GIS) environment and interpolated using the Geostatistical Kriging method to generate continuous concentration surfaces. Kriging was selected because it accounts for spatial autocorrelation among sampling points and provides statistically optimized estimates of pollutant levels across unsampled locations. The interpolation assumed spatial autocorrelation, validated through semi-variogram modeling (spherical model fit; R2 > 0.80).

ArcGIS is a geographic information system that aids in the integration of geographical data and atmospheric dispersion equations. ARC-GIS input incorporates meteorological and topographical data such as temperature, average wind speed, and wind direction. The size of the emission source and other patterns were also distinguished. The Gaussian model limitations and accepted assumptions regarding the source characteristics were assumed during the assessment following the work of Tyovenda *et al.* [8]. In addition, all the predicted surfaces were cross-compared with observed point measurements to verify spatial consistency.

Meteorological parameters, including wind speed, wind direction, temperature and relative humidity, were considered to interpret dispersion behaviour and seasonal variability. Wind direction helped identify dominant transport pathways from the flare stack, while wind speed was used to assess atmospheric dilution potential.

Model inputs included:

- Geographic coordinates of sampling locations.
- Measured seasonal pollutant concentrations.
- Flare stack location as the primary emission source.
- Seasonal meteorological data for the study area.

Model validation was performed by comparing predicted concentration surfaces with observed field measurements at monitoring locations to confirm consistency in spatial trends. This GIS-based geostatistical approach enabled detailed visualization of pollutant dispersion gradients and identification of zones with elevated exposure risk.

G. Air Quality Index (AQI) Calculation Procedure

An estimate of how polluted air is or is expected to get is called the AQI. The AQI and the corresponding risk to public health increased in tandem with air pollution levels. AQI also serves as a foundation for regulatory action and air quality management, and thus assists sensitive groups in making health-protective decisions regarding outdoor activities [31].

The AQI calculations for the Unyenge, Nigeria gas flare stack dataset (2023–2025) presented in this study were carried out following the EPA-454/B-24-002 guidelines/recommendations as presented in Eq. (1) for each pollutant.

$$AQI = \frac{I_{high}-I_{low}}{C_{high}-C_{low}} \times C - C_{low} + I_{low} \quad (1)$$

where C represents the pollutant concentration (e.g., NO_2 in ppm, $PM_{2.5}$ in μg/m^3), C_{high} and C_{low} denote the concentration breakpoints for the pollutant, and I_{high} and I_{low} correspond to the respective AQI breakpoints [30].

H. Statistical Analysis

One-way Analysis of Variance (ANOVA) was conducted using SPSS Version 25.0. Statistical significance was set at $\alpha = 0.05$. Before conducting parametric comparisons, a preliminary assumption test was conducted using the Shapiro-Wilk normality test (W), and Tukey's Honestly Significant Difference (HSD) test was performed after the ANOVA results to verify the significant differences observed between the quarterly seasons as shown by the ANOVA. Additionally, Levene's test (F) was applied to assess equality of variances across seasons.

These statistics are defined as Eq. (2).

$$W = \frac{\left(\sum_{i=1}^{n} a_i x(i)\right)^2}{\sum_{i=1}^{n}(x_i-\bar{x})^2} \quad (2)$$

where $x(i)$ is the ordered sample values, $\bar{x}$ is the samples mean, a_i are the constant derived from covariant matrix of normal distribution and n is the sample size. As a rule, $p < 0.05$ means deviation from normality while $p > 0.05$ means the data are normally distributed, and Eq. (3) gives HSD as:

$$HSD = q \times \sqrt{\frac{MS_{within}}{n}} \quad (3)$$

where q is the studentized range value, MS_{within} is the mean square within group, and n is the sample size per group.

To further test the sample size effect, we calculate η^2 as Eq. (4).

$$\eta^2 = \frac{SS_{between}}{SS_{total}} \quad (4)$$

where $SS_{between}$ is the sum of squares between groups and SS_{total} is the total sum of squares which is the total variation of the entire dataset. Finally, the Levene's test (F) is given by Eq. (5).

$$F = \frac{(N-K)}{(K-1)} \times \frac{\sum_{i=1}^{K} n_i(\bar{z}_{i\cdot}-\bar{Z}_{\cdot\cdot})^2}{\sum_{i=1}^{K}\sum_{j=1}^{n_i}(Z_{ij}-\bar{z}_{i\cdot})^2} \quad (5)$$

where K is the number of different groups being compared, N is the total number of observations across all groups, n_i is the number of observation in the i-th group, Z_{ij} is the absolute deviation of Y_{ij} from it group center, Y_{ij} is the value of j-th observation from the i-th group, $\bar{z}_{i\cdot}$ is the mean of the Z_{ij} for group i, and $\bar{Z}_{\cdot\cdot}$ is the grand mean of all Z_{ij} respectively.

I. Sampling Limitations

The sampling and calibration were conducted on a quarterly basis (Q1 = January–March, Q2 = April–June, Q3 = July–September, and Q4 = October–December), and so continuous calibration and long-term data were challenging due to the time factor and high cost of equipment, continuous monitoring, and calibration. Hence, the findings of this study may be considered preliminary and/or indicative assessment that will provide useful comparative insights for continues monitoring of the gas flaring areas and not for regulatory-level assessment.

III. Result and Discussion

Tables 3–5 and Fig. 5 present the pollutant and meteorological factor results near the gas flare stack in the study area.

Table 3. Quarterly assessment of criteria pollutants and meteorological factors near gas flare stack (2023) at Unyenge, Mbo LGA, Nigeria

Quarter	Dist. (m)	NO_2 (ppm)	SO_2 (ppm)	CO (ppm)	$PM_{2.5}$ (µg/m³)	PM_{10} (µg/m³)	Temp. (°C)	Rel. Hum. (%)	Wind Speed (m/s)	Wind Direction
Q1	60	4.0	6.0	60.0	300.0	480.0	36.8	59.2	1.22	45° NE
	200	3.0	4.0	55.0	270.0	320.0	36.7	59.5	1.13	71° ENE
	500	1.0	3.0	30.0	215.0	280.0	36.4	59.8	0.75	137° SE
Q2	60	2.0	3.0	25.0	125.0	225.0	27.7	70.3	1.50	24° NE
	200	2.0	2.0	23.0	118.0	219.0	27.5	70.3	1.25	80° ENE
	500	0.5	0.7	18.0	101.0	180.0	27.2	70.4	1.04	166° SE
Q3	60	2.0	4.0	22.0	80.0	157.0	26.6	81.4	1.04	38° NE
	200	2.0	3.0	20.0	75.0	129.0	26.4	81.3	1.18	75° ENE
	500	0.3	0.5	8.0	47.0	105.0	26.3	81.3	0.31	157° SE
Q4	60	1.0	2.0	10.0	60.0	139.0	27.4	79.7	1.22	40° NE
	200	2.0	3.0	15.0	80.0	147.0	29.5	69.8	1.09	77° ENE
	500	2.3	1.0	18.0	92.0	166.0	29.7	69.8	0.93	153° SE

Table 4. Quarterly assessment of criteria pollutants and meteorological factors near gas flare stack (2024) at Unyenge, Mbo LGA, Nigeria

Quarter	Dist. (m)	NO_2 (ppm)	SO_2 (ppm)	CO (ppm)	$PM_{2.5}$ (µg/m³)	PM_{10} (µg/m³)	Temp. (°C)	Rel. Hum. (%)	Wind Speed (m/s)	Wind Direction
Q1	60	7.0	10.0	65.0	310.0	495.0	35.6	62.4	0.75	56° NE
	200	5.0	7.0	61.0	300.0	367.0	35.5	62.3	1.04	78° ENE
	500	3.0	5.0	33.0	240.0	283.0	35.3	62.4	0.50	161° SE
Q2	60	1.8	2.0	22.0	158.0	275.0	26.8	76.5	1.22	40° NE
	200	1.5	2.0	20.0	139.0	252.0	26.6	76.3	1.13	70° ENE
	500	0.5	0.5	15.0	116.0	194.0	26.3	76.3	0.75	138° SE
Q3	60	1.0	1.0	10.0	52.0	125.0	25.7	86.5	1.00	24° NE
	200	1.0	1.0	10.0	50.0	117.0	25.5	86.4	1.04	75° ENE
	500	0.2	0.3	5.0	44.0	100.0	25.4	86.2	0.47	143° SE
Q4	60	1.0	1.0	8.0	45.0	118.0	26.8	75.4	1.50	50° NE
	200	3.0	3.0	17.0	115.0	225.0	30.2	65.3	1.13	80° ENE
	500	2.0	1.5	15.0	110.0	209.0	30.0	63.3	0.75	147° SE

Table 5. Quarterly assessment of criteria pollutants and meteorological factors near gas flare stack (2025) at Unyenge, Mbo LGA, Nigeria

Quarter	Dist. (m)	NO_2 (ppm)	SO_2 (ppm)	CO (ppm)	$PM_{2.5}$ (µg/m³)	PM_{10} (µg/m³)	Temp. (°C)	Rel. Hum. (%)	Wind Speed (m/s)	Wind Direction
Q1	60	10.0	13.0	70.0	330.0	498.0	37.4	58.7	1.22	43° NE
	200	8.0	10.0	68.0	311.0	415.0	37.3	58.5	1.18	73° ENE
	500	2.0	5.0	37.0	280.0	305.0	36.7	58.4	0.86	144° SE
Q2	60	5.0	7.0	50.0	210.0	320.0	27.5	70.7	1.50	60° NE
	200	4.0	5.0	38.0	180.0	288.0	27.3	71.8	1.09	82° ENE
	500	2.0	3.0	25.0	126.0	265.0	27.8	70.5	0.86	158° SE

The results of the Quarterly assessment of the criteria pollutants (NO_2, SO_2, CO, $PM_{2.5}$, and PM_{10}) and meteorological factors near a gas flare stack in Unyenge, Mbo LGA, Nigeria, from 2023 to 2025 are presented in Tables 3–5, and Fig. 5 reveals significant air quality challenges. Measurements at 60 m, 200 m, and 500 m from the flare stack highlight spatial and temporal trends driven by the flare stack emissions and meteorological conditions, similar to the findings of Nwosisi *et al.* [20].

Pollutant concentration trends were observed, showing NO_2 concentrations peaked at 10.0 ppm in Q1 of 2025 at 60 m from the flare stack and dropped to 0.2 ppm in Q3 of 2024 at 500 m from the flare stack. SO_2 reached 13.0 ppm in Q1 of 2025 at 60 m away from the flare stack, with a lowest value of 0.3 ppm occurring in Q3 of 2024 at 500 m from the flare stack. CO hit 70.0 ppm in Q1 of 2025 at 60 m, while $PM_{2.5}$ and PM_{10} peaked at 330.0 µg/m³ and 498.0 µg/m³ in Q1 of 2025 at 60 m from the stack, with lower values of 44.0 µg/m³ and 100.0 µg/m³ occurring in Q3 of 2024 at 500 m, respectively. All pollutants showed a clear decline with increasing distance, confirming that the flare stack was the primary source. A closer look showed that the highest

concentrations occurred in Q1 (dry season) across all years, likely due to low humidity (58.4–62.4%) and reduced atmospheric mixing, which limits dispersion. Q3 (wet season) consistently showed the lowest levels, attributed to high humidity (81.3–86.5%) and wet deposition. Q4 exhibited moderate concentrations reflecting transitional weather patterns. Exceptional patterns were occasionally observed, with higher $PM_{2.5}$ at 500 m than at 200 m in Q4 2024 (110.0 vs. 115.0 µg/m³), and this variation may be attributed to temporal influences from local sources or wind patterns.

For the meteorological factors, it was observed that the temperatures ranged from 25.4 °C (Q3 2024, 500 m) to 37.4 °C (Q1 2025, 60 m), with slight increases near the flare stack, possibly due to radiated heat. Relative humidity (Rel.) was lowest in Q1 (58.4–62.4%) and highest in Q3 (81.3–86.5%), aligning with the dry and wet seasons. Wind speeds varied from 0.31 m/s (Q3 2023, 500 m) to 1.50 m/s (Q2 2023, Q4 2024, 60 m), with directions shifting from NE (24°–60°) to SE (137°–166°).

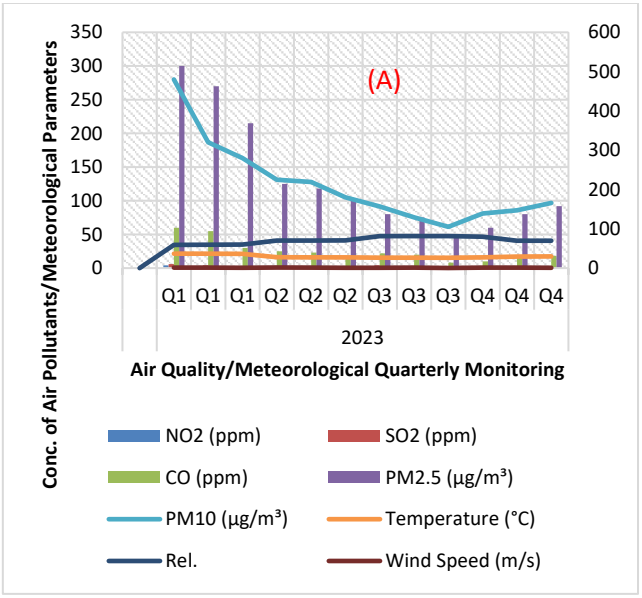

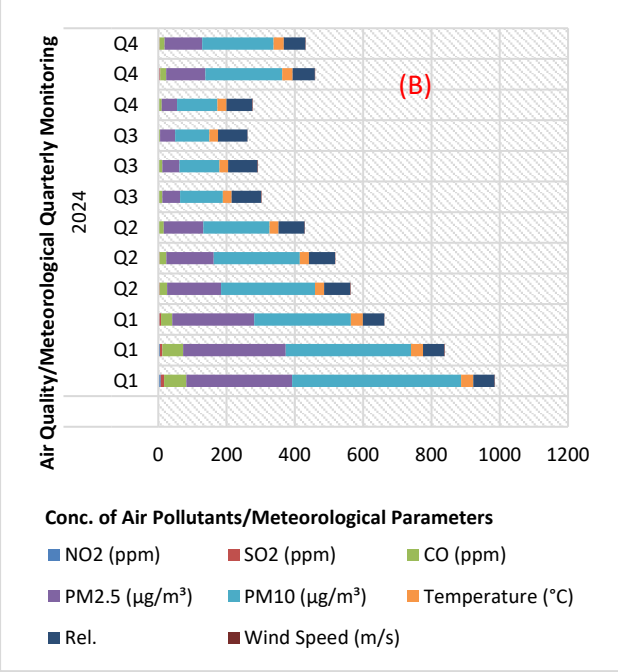

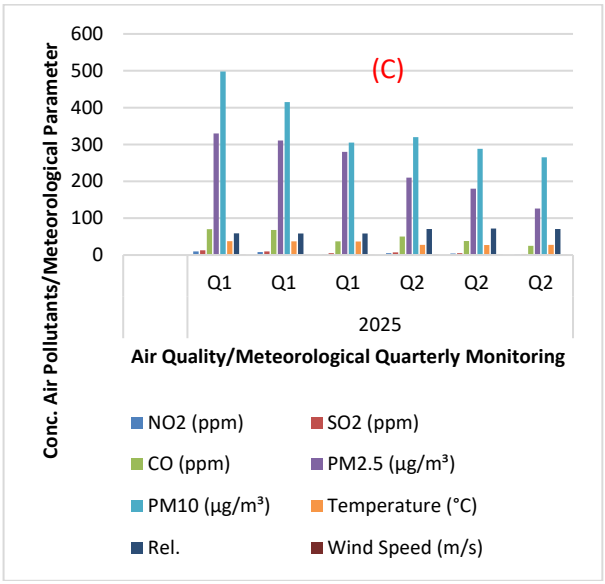

Fig. 5. Air quality/meteorological quarterly monitoring for (A) 2023; (B) 2024; (C) 2025.

It can be seen that low wind speed values in Q3 contributed to the higher values of pollutant accumulation, while higher wind speeds in Q2 and Q4 enhanced dispersion, reducing the pollutant concentrations at 500 m. Wind direction influenced pollutant distribution, with South East (SE) winds carrying emissions away from farther measurement points. These findings align with research indicating that meteorological factors such as wind speed and humidity significantly influence pollutant dynamics in Nigeria's seasonal and annual patterns [7, 8]. Q1 consistently showed elevated pollutant levels owing to dry conditions, with 2025 exhibiting the highest concentrations of particulates ($PM_{2.5}$ at 330.0 µg/m³, 60 m). Q2 and Q3, corresponding to the wet season, showed reduced levels, with Q3 2024 recording the lowest particulates ($PM_{2.5}$ at 44.0 µg/m³, 500 m).

It was observed from all the results that the Q4 levels were moderate and variable. This may be due to shifting weather patterns and climate change. Annual trends indicated a slight increase in peak concentrations from 2023 to 2025, particularly in Q1, suggesting potential increases in flare activity or reduced dispersion efficiency around the study area. The spatial analysis of the pollutants is presented in Fig. 6.

In Fig. 6, the dispersion models for criteria pollutants around the Flare Stack (FS) and Early Processing Facility (EPF) reveal significant air quality concerns with implications for human health, environmental management, and regulatory compliance. However, extremely high pollutant concentrations are capped at an AQI value of 500, which may underestimate the severity of extreme exposure levels. Notably, Ambient Air Quality Index (AQI) represents air quality monitoring during the first quarter, corresponding to the dry season (harmattan period) from November through March. This seasonal condition is associated with elevated levels of suspended particulate matter alongside gaseous air pollutants.

Nitrogen dioxide (NO_2) exhibited the highest concentrations, ranging from 2.57 to 3.15 ppm, at the FS and EPF, while the lowest concentrations, ranging from 1.38 to 1.97 ppm, were observed outside the EPF. These elevated NO_2 levels near facilities pose risks of respiratory and

cardiovascular issues for workers and nearby communities, particularly in high-concentration zones.

Sulfur dioxide (SO_2) showed peak concentrations northward of the FS and EPF, ranging from 3.59 to 4.49 ppm (marked in red), decreasing southward to 2.05–3.14 ppm outside the EPF. These levels, especially northward, suggest the potential for acid rain, which could harm immediate ecosystems, including vegetation and water bodies. Spatial variation indicates wind-driven dispersion, which increases exposure risk in northern areas.

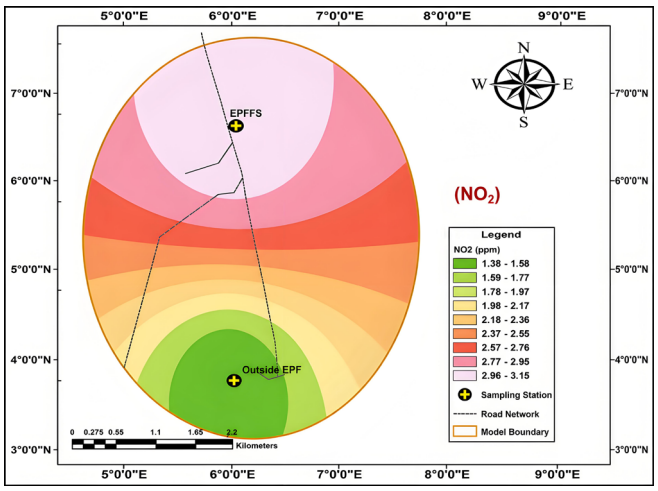

(a)

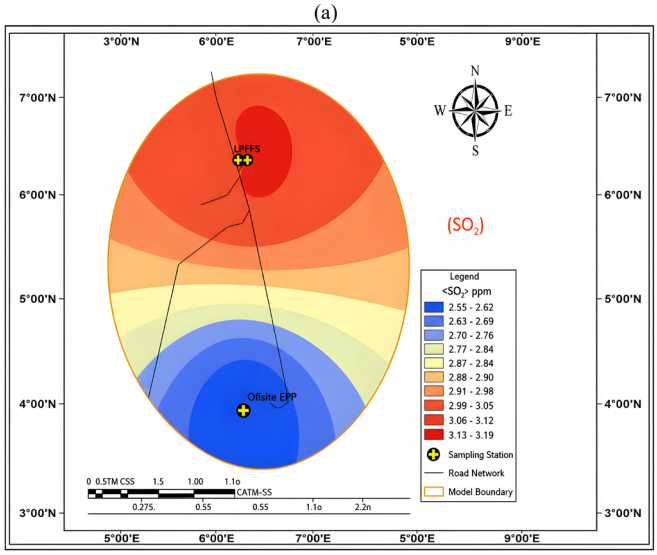

(b)

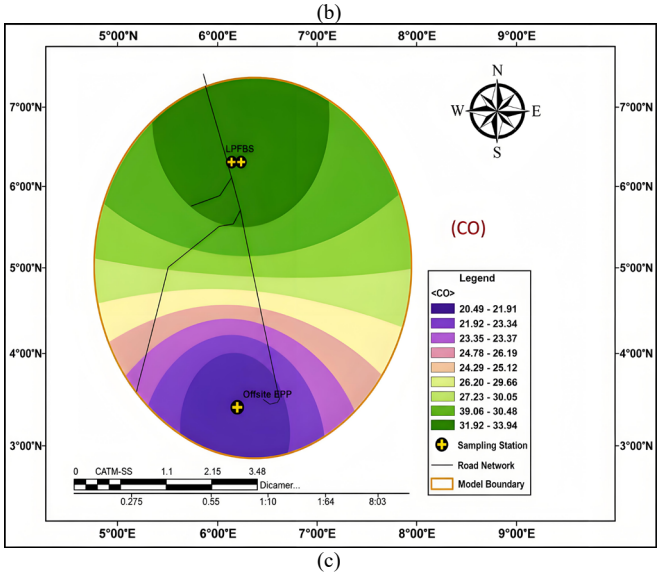

(c)

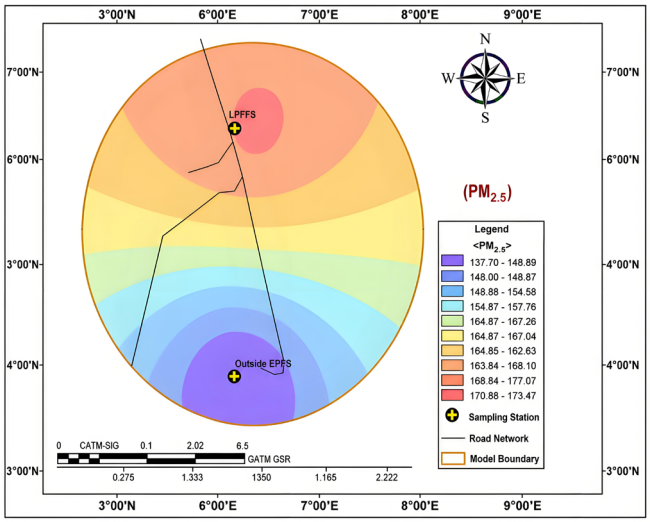

(d)

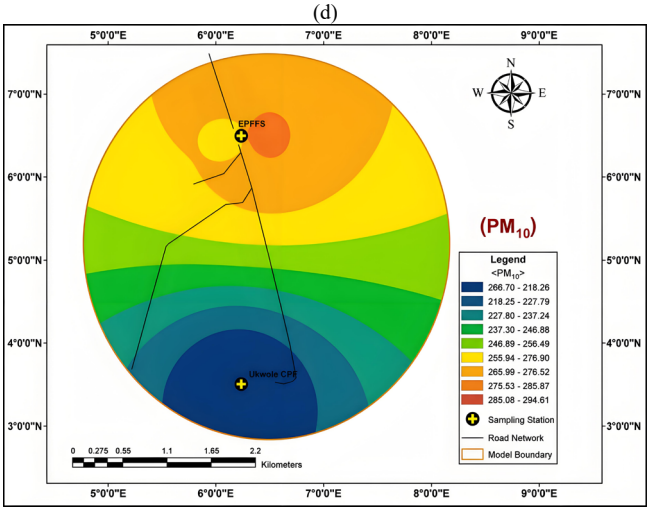

(e)

Fig. 6. Spatial analysis of criteria pollutants. (a) NO_2, (b) SO_2, (c) CO, (d) $PM_{2.5}$, (e) PM_{10}.

Carbon monoxide (CO) concentrations were higher northward of the FS, EPF, and surrounding areas, ranging from 29.47 to 33.98 ppm, with the lowest concentrations, between 20.40 and 26.459 ppm, recorded outside the EPF. These elevated CO levels near the facilities could contribute to health risks, including reduced oxygen delivery in the body, particularly for sensitive populations, such as babies and the elderly.

Particulate matter spatial analysis revealed that $PM_{2.5}$ concentrations were lowest outside the EPF, ranging from 137.1–148.77 μg/m³, while the highest levels were recorded at the FS and EPF, ranging from 164.31–172.07 μg/m³. Similarly, PM_{10} concentrations peaked at the FS and EPF, ranging from 266.99–294.61 μg/m³, with the lowest levels outside the EPF, between 208.7 and 237.34 (Fig. 5). These $PM_{2.5}$ and PM_{10} levels significantly exceeded the air quality standards (WHO guidelines: 15 μg/m³ annual mean for $PM_{2.5}$, 45 μg/m³ for PM_{10}), revealing the tendency of non-compliance with regulations and the potential health risks due to their ability to penetrate deep into the lungs [21, 32, 33]. In addition, high particulate concentrations can reduce visibility and contribute to environmental degradation through deposition [29, 34].

To calculate the Air Quality Index (AQI) for the data at the gas flare stack in Unyenge, Mbo LGA, Nigeria, from 2023 to 2025, the AQI was calculated for each pollutant (NO_2, SO_2,

CO, $PM_{2.5}$, PM_{10}) based on their concentrations according to Eq. (1). The highest AQI value among the pollutants for a given time and location determines the overall AQI. The AQI breakpoints for the pollutants in the dataset are presented in Tables 6–10 for all the pollutants considered.

Table 6. NO_2 (1 h average, ppm)

AQI Category	AQI Range	NO_2 (ppm)
Good	0–50	0–0.053
Moderate	51–100	0.054–0.1
Unhealthy for Sensitive Groups	101–150	0.101–0.36
Unhealthy	151–200	0.361–0.649
Very Unhealthy	201–300	0.65–1.249
Hazardous	301–500	1.25–2.049

Table 7. SO_2 (1 h average, ppm)

AQI Category	AQI Range	SO_2 (ppm)
Good	0–50	0–0.035
Moderate	51–100	0.036–0.075
Unhealthy for Sensitive Groups	101–150	0.076–0.185
Unhealthy	151–200	0.186–0.304
Very Unhealthy	201–300	0.305–0.604
Hazardous	301–500	0.605–1.004

Table 8. CO (8 h average, ppm)

AQI Category	AQI Range	CO (ppm)
Good	0–50	0–4.4
Moderate	51–100	4.5–9.4
Unhealthy for Sensitive Groups	101–150	9.5–12.4
Unhealthy	151–200	12.5–15.4
Very Unhealthy	201–300	15.5–30.4
Hazardous	301–500	30.5–50.4

Table 9. $PM_{2.5}$ (24 h average, μg/m³)

AQI Category	AQI Range	$PM_{2.5}$ (μg/m³)
Good	0–50	0–12.0
Moderate	51–100	12.1–35.4
Unhealthy for Sensitive Groups	101–150	35.5–55.4
Unhealthy	151–200	55.5–150.4
Very Unhealthy	201–300	150.5–250.4
Hazardous	301–500	250.5–500.4

Table 10. PM_{10} (24 h average, μg/m³)

AQI Category	AQI Range	PM_{10} (μg/m³)
Good	0–50	0–54
Moderate	51–100	55–154
Unhealthy for Sensitive Groups	101–150	155–254
Unhealthy	151–200	255–354
Very Unhealthy	201–300	355–424
Hazardous	301–500	425–604

A Sample calculation for the 2023 Q1 at a distance of 60 m is as follows:

- NO_2: 4.0 ppm

This exceeds the highest breakpoint (2.049 ppm, AQI 500). Because the concentration was significantly above the hazardous range, the AQI was capped at 500.

- SO_2: 6.0 ppm

This exceeds the highest breakpoint (1.004 ppm, AQI 500). AQI = 500.

- CO: 60.0 ppm

The highest breakpoint (50.4 ppm, AQI 500) is observed. AQI = 500.

- $PM_{2.5}$: 300.0 μg/m³

Falls in the Hazardous range (250.5–500.4 μg/m³, AQI 301–500).

AQI = 500 – 301/500.4 – 250.5 × (300.0 – 250.5) + 301 = 199/249.9 ×49.5 + 301 = 340.4

- PM_{10}: 480.0 μg/m³

Falls in the Hazardous range (425–604 μg/m³, AQI 301–500).

AQI = 500 – 301/604 – 425 × (480.0 – 425) + 301 = 199/179 = 362.2

Overall AQI: Max (500, 500, 500, 340.4, 362.2) = 500 (Hazardous).

Table 11. Summary air quality index (AQI)

Year	Quarter	Distance (m)	NO_2 AQI	SO_2 AQI	CO AQI	$PM_{2.5}$ AQI	PM_{10} AQI	Overall AQI	AQI Category
2023	Q1	60	500	500	500	340.4	362.2	500	Hazardous
2023	Q1	200	500	500	500	318.0	302.2	500	Hazardous
2023	Q1	500	151	500	302.0	239.8	260.8	500	Hazardous
2023	Q2	60	271	500	151	199.2	211.6	500	Hazardous
2023	Q2	200	271	283	141.4	187.6	205.2	283	Very Unhealthy
2023	Q2	500	76	94	110.2	161.2	168.8	161.2	Unhealthy
2023	Q3	60	271	500	135.8	128.8	145.2	500	Hazardous
2023	Q3	200	271	500	126.2	120.0	116.4	500	Hazardous
2023	Q3	500	50	67	50	75.2	91.6	91.6	Moderate
2023	Q4	60	151	283	62.6	96.0	127.6	283	Very Unhealthy
2023	Q4	200	271	500	94.6	128.8	135.6	500	Hazardous
2023	Q4	500	304	134	110.2	147.2	153.2	304	Hazardous
2024	Q1	60	500	500	500	247.6	398.8	500	Hazardous
2024	Q1	200	500	500	500	239.8	349.8	500	Hazardous
2024	Q1	500	500	500	303.8	191.6	263.2	500	Hazardous
2024	Q2	60	245	283	135.8	250.8	260.0	283	Very Unhealthy
2024	Q2	200	202	283	126.2	222.8	237.6	283	Very Unhealthy
2024	Q2	500	76	67	94.6	184.8	181.6	184.8	Unhealthy
2024	Q3	60	151	134	62.6	83.2	113.2	151	Unhealthy
2024	Q3	200	151	134	62.6	80.0	106.8	151	Unhealthy
2024	Q3	500	38	50	50	70.4	92.0	92.0	Moderate
2024	Q4	60	151	134	50	72.0	107.6	151	Unhealthy
2024	Q4	200	500	500	103.8	183.2	211.6	500	Hazardous
2024	Q4	500	271	201	94.6	176.0	197.2	271	Very Unhealthy
2025	Q1	60	500	500	500	263.6	398.8	500	Hazardous
2025	Q1	200	500	500	500	255.6	391.6	500	Hazardous
2025	Q1	500	271	500	312.2	223.6	287.6	500	Hazardous
2025	Q2	60	500	500	500	327.6	302.4	500	Hazardous
2025	Q2	200	500	500	234.2	287.6	271.2	500	Hazardous
2025	Q2	500	271	500	151.0	201.2	250.0	500	Hazardous

The AQI values for each quarter, year, and distance are summarized in Tables 6–10. The air quality ranges from moderate (e.g., 2023 Q3 at 500 m, AQI = 91.6) to hazardous (e.g., 2023 Q1 at 60 m, AQI = 500), with closer distances

(60 m and 200 m) and Q1 periods showing the worst air quality scenario, often driven by high NO_2, SO_2, and CO concentrations.

Fig. 7 presents the overall AQI by distance and quarter for 2023–2025. Table 11 presents a summary of the AQI.

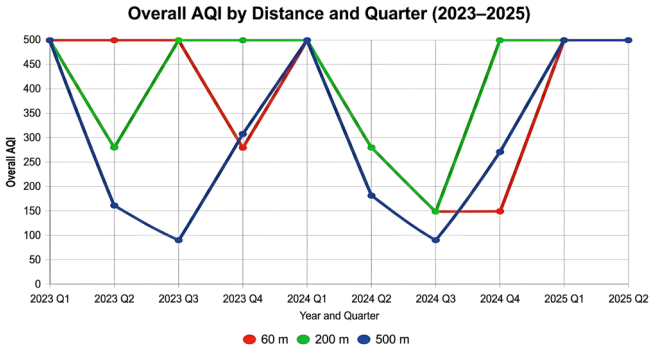

Fig. 7. Overall AQI by distance and quarter (2023–2025).

The line chart in Fig. 7 shows that the AQI values consistently peaked at 60 and 200 m from the flare stack, often reaching 500 (most hazardous), particularly in Q1 and Q4 of each year (Fig. 7). The 500 m distance shows more variability, with lower AQI values in Q3 2023 (91.6, moderate) and Q3 2024 (92, moderate), indicating better air quality far from the flare stack. Some results showed higher pollution levels in the first quarter (AQ1) and lower levels in the third quarter (AQ3)—appear repeatedly and could be streamlined. As explained earlier, the first quarter corresponds to the dry season, which favors the accumulation of suspended particulate matter and gaseous emissions, including those from flare stacks. In contrast, the third quarter falls within the rainy season, when wet deposition (rainfall scavenging pollutants from the atmosphere) leads to reduced pollution levels. This seasonal contrast explains the consistently higher pollutant concentrations in the dry period and lower levels during the wet season.

The bar chart in Fig. 8 shows that NO_2, SO_2, and CO frequently drive the AQI to 500 at 60 m, particularly in Q1 and Q2 of each year (Fig. 8). $PM_{2.5}$ and PM_{10} contribute significantly but are less dominant, with AQI values typically in the Unhealthy to Hazardous range.

Similarly, in Fig. 6, the Air Quality Index (AQI) by Pollutant at 60 m (2023–2025) is presented.

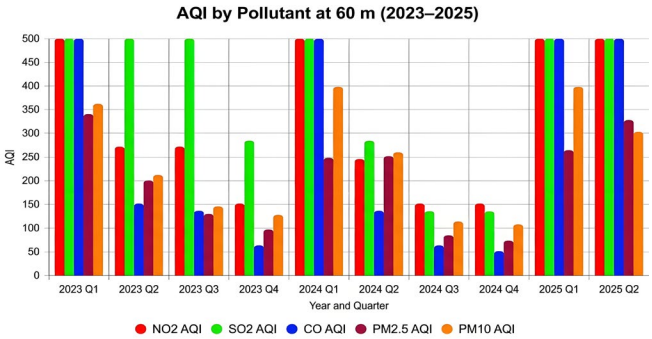

Fig. 8. Air quality index (AQI) by pollutant at 60 m (2023–2025).

A further test to confirm the distance, quarterly and seasonal variability of the pollutant levels across all the sampled points was conducted using relevant statistical tools, and the results are presented in Table 12.

Based on the data in Table 12, both seasonal and spatial factors significantly influence pollutant concentrations, though seasonal dynamics exert the dominant control. Statistical rigor was maintained through the Shapiro-Wilk and Levene's tests, which confirmed normal distribution and homogeneity of variance (p_s and $p_d > 0.005$). These results validated the use of parametric ANOVA, ensuring the reliability of the subsequent inferences and minimizing the risk of statistical errors.

Table 12. Summary of statistical tests for seasonal and distance effects on pollutant concentrations (2023–2025)

Pollutant	Shapiro Wilk (P)	Levene's Test (P)	Seasonal ANOVA F (df)	p_s-value	η_s^2	Distance ANOVA F (df)	p_d-value	η_d^2	Tukey Post-hoc (Season)	Effect Magnitude
CO	0.318	0.412	14.6 (3, 32)	<0.001	0.58	9.8 (2, 33)	0.001	0.37	Q1 > Q2, Q3, Q4	Very Large
NO_2	0.276	0.395	12.8 (3, 32)	<0.001	0.52	7.4 (2, 33)	0.003	0.31	Q1 > Q3, Q4	Large
SO_2	0.241	0.368	11.5 (3, 32)	<0.001	0.49	6.9 (2, 33)	0.004	0.29	Q1 > Q3	Large
$PM_{2.5}$	0.347	0.421	18.2 (3, 32)	<0.001	0.63	10.6 (2, 33)	<0.001	0.39	Q1 > All others	Very Large
PM_{10}	0.259	0.403	16.4 (3,32)	<0.001	0.60	9.2 (2, 33)	0.001	0.35	Q1 > Q2, Q3	Very Large

All pollutants showed highly significant seasonal variation ($p_s < 0.001$) with substantial effect sizes ($\eta_s^2 = 0.49 - 0.63$). In environmental science, these values are considered large, indicating that seasonality explains 49% to 63% of the total concentration variability. The most profound seasonal impact was observed in $PM_{2.5}$ ($\eta_s^2 = 0.63$), followed by PM_{10} and CO. Post-hoc Tukey comparisons identified Q1 (Dry/Harmattan) as the period with significantly higher concentrations across all pollutants. This peak is likely attributed to the ground-level emissions of horizontal flare stack, which have been reported to limit pollutant dispersion, and the unique West African meteorology during Harmattan, where reduced precipitation, lower mixing heights, and atmospheric stability lead to pollutant accumulation rather than dispersion [31–34]. This suggests a synergistic interaction between gas flaring emissions and seasonal atmospheric stagnation.

Spatial factors also showed statistical significance ($p_d \leq 0.004$), confirming a clear radial decay from 60 m to 500 m. While the spatial effect sizes ($\eta_d^2 = 0.29 - 0.39$) were moderate to large, they were notably lower than seasonal effects. This implies that while proximity to the flare stack is a major risk factor, atmospheric conditions play a more critical role in determining concentration levels in agreement with the findings of Chen *et al.* [35]. The decay pattern aligns with Gaussian plume dispersion theory, highlighting that residents within 200 m face significantly higher exposure than those at 500 m.

Pollutant-specific analysis revealed that CO and NO_2 are highly sensitive to dispersion conditions, with CO

specifically reflecting incomplete combustion during flare intensity fluctuations [8, 29, 36, 37]. SO_2 concentrations also peaked during Q1, suggesting meteorological confinement of sulfur-containing hydrocarbon emissions [29, 38, 39]. Particulate matter showed the strongest seasonal dependence; the massive effect size for $PM_{2.5}$ suggests that two-thirds of its variability stems from the combination of direct flaring, secondary aerosol formation, and Harmattan dust entrainment [21, 37, 38].

Ultimately, these statistical tests reveal a critical insight that atmospheric dynamics exert greater control over pollutant variability than radial proximity. In reality, the meaning is that communities may face higher risks during the Harmattan season even at greater distances [39, 40]. Given the known links between particulate matter and cardiopulmonary morbidity, these seasonal spikes represent a major public health concern [41]; thus, mitigation strategies must prioritize combustion efficiency, enhanced monitoring during the dry season, and the strict enforcement of buffer zones around flare sites.

In Comparison with global studies, our findings align with the work of Johnson and Coderre [3] in Alberta, Canada, who reported NO_2 and Particulate Matter (PM) hotspots near flares, and Abdul-Wahab *et al.* [40] in Iraq, where SO_2 levels near flares exceeded 5 ppm, similar to Unyenge. These pollutants pose significant risks, including respiratory issues (CO and PM), cardiovascular effects (NO_2), and acid rain (SO_2) [40, 41]. Acid rain is created when gas flares further burn in the humid atmosphere, particularly offshore, and has corrosive properties that can cause surface water pollution, unpleasant effects on flora, and widespread environmental devastation, including freshwater, coastal, and mangrove ecosystems [42–44]. High PM levels also suggest soot-related soil and water contamination, as reported by Ite and Ibok [45].

AQI values at 60 m and 200 m often reached 500 (hazardous) in Q1 owing to high NO_2, SO_2, CO, $PM_{2.5}$, and PM_{10}, improving to Moderate at 500 m and in Q3/Q4, reflecting reduced risks with distance and during wet seasons.

The ANOVA Q3 and Q4 mean values suggest reduced flaring or better dispersion, whereas Q2's intermediary mean signifies moderate flaring. These results support the work of [45, 46] on gas flaring-related PM, NO_2, and SO_2 health impacts in the USA.

Manisalidis *et al.* [44] advocated global emission controls, complementing Unyenge's call for vertical stacks and flaring regulations to reduce health risks. It has been suggested that all the unhealthy pollutant levels captured be mitigated with strategies such as gas capture technologies, enhanced flare efficiency, expanded real-time monitoring, and community health advisories during high-pollution periods.

IV. Conclusion

Seasonal assessment of pollutants emitted from flared stacks and meteorological factors was conducted at specified locations to assess the impact of gas flaring on air quality and public health in the Southeastern City of Unyenge-Mbo. The pollutants monitored exceeded the World Health Organization's safe levels, putting human health and the environment at risk.

At approximately 60 m from the flare stack, criteria pollutants such as NO_2, SO_2, CO, $PM_{2.5}$, and PM_{10} were at high risk levels. Notably, SO_2 peaked at 13.0 ppm, and $PM_{2.5}$ was at 498 μg/m³, which is twice the WHO guideline limit for a 24 h period. The results demonstrate that both season and distance significantly influence pollutant concentrations; however, seasonal variability exerts the dominant control.

One-way ANOVA revealed highly significant seasonal effects for all pollutants ($p_s < 0.001$), with very large effect sizes for $PM_{2.5}$ ($\eta_s^2 = 0.63$), PM_{10} ($\eta_s^2 = 0.60$), and CO ($\eta_s^2 = 0.58$), and large effects for NO_2 ($\eta_s^2 = 0.52$) and SO_2 ($\eta_s^2 = 0.49$). These findings indicate that 49–63% of total concentration variability is attributable to seasonal atmospheric dynamics.

Post-hoc analysis consistently identified the dry/Harmattan season (Q1) as the period of maximum pollutant accumulation. Distance-based ANOVA further confirmed significant radial decay ($p_d \leq 0.004$; $\eta_d^2 = 0.29–0.39$), demonstrating elevated exposure within 200 m of the flare stack. However, seasonal effects were stronger than proximity effects, highlighting the critical role of atmospheric stability and reduced dispersion during dry-season conditions.

Particulate matter exhibited the greatest seasonal amplification, suggesting heightened cardiopulmonary exposure risk during Harmattan. Overall, the findings underscore the need for seasonally targeted monitoring, improved flare combustion efficiency, and enforcement of buffer zones to mitigate exposure in flare-affected communities.

It was observed that air quality was greatly affected by seasonal variations, with Q1 being the worst because of the emotional impact of the dry season and increased stack activity. ANOVA analysis showed that the levels of pollutants were considerably lower in Q3, Q4, and Q2. Q2 was superior to Q4, whereas Q1 had the highest. However, during the course of the investigation, the pollutants were never at a safe level. Additionally, the AQI remained dangerous throughout the entire time period, often reaching 500 (maximum danger), which is considered the most aggressive impact.

It is recommended that routine monitoring be carried out in the entire Niger Delta to create more public awareness, and that the Nigerian government should regulate the issue with the urgency it deserves through enhanced policy guidelines. Otherwise, the hazardous conditions in Unyenge will persist, perpetuate health crises, and cause ecological degradation.

Conflict of Interest

The authors declare no conflict of interest.

Author Contributions

T.J.A. contributed to the study conception design, methodology, data curation, perform the analysis, writing and reviewing of the manuscript, I.S.A. contributed to conception, methodology, data analysis, resources, validation, wrote the original draft. U.U.S. performed the data analysis and reviewed the manuscript, visualized the manuscript. S.I.I. visualized and reviewed the manuscript. All the authors have read and agreed to the final version of the manuscript.

ACKNOWLEDGMENT

The authors express deep gratitude for the support and collaboration from our respective university administrations, especially for providing the essential computational resources that enabled this research.

REFERENCES

[1] T. E. Ologunorisa, "A review of the effects of gas flaring on the Niger Delta environment," *International Journal of Sustainable Development and World Ecology*, vol. 8, no. 3, pp. 249–255, 2001.

[2] O. E. Orisakwe, "Crude oil and public health issues in Niger Delta, Nigeria: Much ado about the inevitable," *Environmental Research*, vol. 194, 110725, 2001.

[3] M. R. Johnson and A. R. Coderre, "An analysis of flaring and venting activity in the Alberta upstream oil and gas industry," *Journal of the Air and Waste Management Association*, vol. 61, no. 2, pp. 190–200, 2011.

[4] C. D. Elvidge, M. Zhizhin, K. Baugh *et al.*, "Methods for global survey of natural gas flaring from visible infrared imaging radiometer suite data," *Energies*, vol. 9, no. 1, 14, 2016.

[5] 2024 Global gas flaring tracker report (GGFTR). [Online]. Available: https://www.worldbank.org/en/programs/gasflaringreduction/publication/2024-global-gas-flaring-tracker-report

[6] G. N. Dappa and V. A. Akujuru, "Impact of gas flare on human life and wellbeing of ogba/egbema/ndoni local government area of rivers state," *European Journal of Environment and Earth Sciences*, vol. 4, no. 2, pp. 32–35, 2023.

[7] I. F. Chizoruo, O. A. Iheanyichukwu, N. P. Chukwuemeka *et al.*, "Ambient air quality assessment of Orlu, Southeastern, Nigeria," *Journal of Applied Sciences*, vol. 17, no. 9, pp. 441–457, 2017.

[8] A. A. Tyovenda, T. J. Ayua, and T. Sombo, "Modeling of gaseous pollutants (CO and NO_2) emission from an industrial stack in Kano city, northwestern Nigeria," *Atmos. Environ.*, vol. 253, 118356, 2021.

[9] K. N. Palani, N. K. Saravanakumar, and P. Ilanagai, "Removal of pollutants using electrooxidation integrated membrane bioreactor: Validation through lumped parameter kinetic modelling, thermodynamic parameter exploration in wastewater treatment," *Total Environment Engineering*, vol. 4, 100032, 2025.

[10] K. H. Jodhani, N. Gupta, A. D. Parmar *et al.*, "Synergizing google earth engine and earth observations for potential impact of land use/land cover on air quality," *Results in Engineering*, vol. 22, 102039, 2024.

[11] R. E. Mootassem, Z. Al-Dawood, and T. Ali, "Spatiotemporal air quality mapping and PM10 modelling in Abu Dhabi City, UAE," *International Journal of Environmental Science and Development*, vol. 15, no. 2, pp. 57–62, 2024.

[12] M. A. Lala, C. S. Onwunzo, O. A. Adesina *et al.*, "Particulate matters pollution in selected areas of Nigeria: Spatial analysis and risk assessment," *Case Studies in Chemical and Environmental Engineering*, vol. 7, 100288, 2023.

[13] M. R. Johnson, L. W. Kostiuk, and J. L. Spangelo, "A characterization of solution gas flaring in Alberta Upstream oil and gas industry," *Journal of the Air & Waste Management Association*, vol. 51, no. 8, pp. 1167–1177, 2001.

[14] A. D. G. Nwosu, E. Ossai, O. Onwuasoigwe *et al.*, "Burnout and presenteeism among healthcare workers in Nigeria: Implications for patient care, occupational health and workforce productivity," *Journal of Public Health in Africa*, vol. 10, no. 1, 2021.

[15] ERCB (2009). ERCB upstream petroleum industry flaring and venting report: Industry performance for year ending December 31, 2009. [Online]. Available: https://archive.org/details/micro_IA40244207_2925

[16] M. C. Nwosisi, O. Oguntoke, and A. M. Taiwo, "Dispersion modeling of PM_{10} from selected flow stations in the Niger Delta, Nigeria: Implications on soot pollution," *Environmental Systems Research*, vol. 10, Art. no. 9, 2021.

[17] O. G. Fawole, X. Cai, O. E. Abiye *et al.*, "Dispersion of gas flaring emissions in the Niger delta: Impact of prevailing meteorological conditions and flare characteristics," *Environmental Pollution*, vol. 246, pp. 284–293, 2019.

[18] C. O. Ehumadu, U. Lucky, and N. B. Onyedikachukwu, "Air pollution assessment of a gas flare site in the Niger Delta Region," *Journal of Engineering Research and Reports*, vol. 20, no. 8, pp. 116–126, 2021.

[19] O. Akpoyibo and O. J. Vwavware, "Assessing the impact of gas flaring activities in Ebedei, Southern Nigeria," *Nigerian Journal of Physics*, vol. 33, no. 2, pp. 137–145, 2024.

[20] M. C. Nwosisi, O. Oguntoke, A. M. Taiwo *et al.*, "Spatial patterns of gas flaring stations and the risk to the respiratory and dermal health of residents of the Niger Delta, Nigeria," *Scientific African*, vol. 12, e00762, 2021.

[21] T. J. Ayua, A. A. Tyovenda, E. V. Tikyaa *et al.*, "Simulation of fine particulate matter dispersion from the grand cereals industry Jos, Nigeria using a modified gaussian plume model," *International Journal of Environmental Science and Development*, vol. 14, no. 2, pp. 111–118, 2022.

[22] K. Thompson, J. Steigerwald, H. Ray *et al.*, "Review of industrial chemicals impacting potable reuse: Hazards, removal, and recommendations for enhanced source control programs," *Total Environment Engineering*, vol. 4, 100027, 2025.

[23] J. Nriagu, E. A. Udofia, I. Ekong *et al.*, "Health risks associated with oil pollution in the Niger Delta, Nigeria," *International Journal of Environmental Research and Public Health*, vol. 13, no. 3, 346, 2016.

[24] A. A. Elijah, "A review of the environmental impact of gas flaring on the physiochemical properties of water, soil and air quality in the Niger Delta Region of Nigeria," *Earthline Journal of Chemical Sciences*, vol. 7, no. 1, pp. 35–52, 2021.

[25] J. P. Esavwede and U. G. Oyibodoro, "Gas flaring in Nigeria's Niger Delta: Legal challenges and lessons from Norway's regulatory framework," *Journal of Environmental Law & Policy*, vol. 5, no. 1, pp. 148–166, 2025.

[26] O. H. Yakubu, "Particle (soot) pollution in port Harcourt Rivers State, Nigeria—Double air pollution burden? Understanding and tackling potential environmental public health impacts," *Environments*, vol. 5 no. 1, 2, 2018.

[27] S. O. Giwa, C. N. Nwaokocha, S. I. Kuye *et al.*, "Gas flaring attendant impacts of criteria and particulate pollutants: A case of Niger Delta Region of Nigeria," *Journal of King Saud University-Engineering Sciences*, vol. 31, no. 3, pp. 209–217, 2019.

[28] MSA Safety. (2018). ALTAIR 5X multigas detector: Instruction manual (Rev. 2). [Online]. Available: http://site.msagasmonitors.com/MSA/pdf/msa-altair-5x_manual.pdf

[29] T. J. Ayua, M. O. Audu, S. I. Ioryue *et al.*, "Meteorological effects on ambient air quality perturbations of some criteria pollutants in northern Nigeria industries," *Discover Environment*, vol. 4, 65, 2026.

[30] USEPA. Technical assistance document for the reporting of daily air quality—The air quality index (AQI). [Online]. Available: https://document.airnow.gov/technical-assistance-document-for-the-reporting-of-daily-air-quailty.pdf

[31] D. N´uñez-Alonso, L. V. P´erez-Arribas, S. Manzoor *et al.*, "Statistical tools for air pollution assessment: Multivariate and spatial analysis studies in the Madrid Region," *Journal of Analytical Methods in Chemistry*, vol. 2019, no. 1, 9753927, 2019.

[32] P. Opas and T. Pajaree, "The inhalation exposure of $PM_{2.5}$ and PM_{10} from traffic exhaust at the Uthai Tani Bus Station and two Roadside Areas in Uthai Tani, Thailand," *International Journal of Environmental Science and Development*, vol. 15, no. 2, pp. 77–81, 2024.

[33] G. João and R. Cerdeira, "Assessing indoor and outdoor PM10 levels in school: Insights from a case study," *International Journal of Environmental Science and Development*, vol. 16, no. 3, pp. 226–233, 2025.

[34] [34] F. C. Ibe, A. I. Opara, C. E. Duru *et al.*, "Statistical analysis of atmospheric pollutant concentrations in parts of Imo State, Southeastern Nigeria," *Scientific African*, vol. 7, Art. no. e00237, 2020.

[35] C. Chen, D. C. McCabe, L. E. Fleischman *et al.*, "Black carbon emissions and associated health impacts of gas flaring in the United States," *Atmosphere*, vol. 13, no. 3, 385, 2022.

[36] S. C. Anenberg, J. Schwartz, D. Shindell *et al.*, "Global air quality and health co-benefits of mitigating near-term climate change through methane and black carbon emission controls," *Environmental Health Perspectives*, vol. 120, no. 6, pp. 831–839, 2012.

[37] S. A. Horn, and P. K. Dasgupta, "The air quality index (AQI) in historical and analytical perspective a tutorial review," *Talanta*, vol. 267, 125260, 2024.

[38] J. A. Sonibare, F. M. Adebiyi, E. O. Obanijesu *et al.*, "Air quality index pattern around petroleum production facilities," *Management of Environmental Quality: An International Journal*, vol. 21, pp. 379–392, 2010.

[39] E. O. Nwaichi, S. E. Uzodike, B. A. Amadi *et al.*, "Ambient particulate matter levels and health profile in residents of Choba and Mgbuoba areas of Rivers State: A cross-sectional study," *Journal of the Air and Waste Management Association*, vol. 71, no. 12, pp. 1472–1482, 2021.

[40] S. A. Abdul-Wahab, S. O. Fadlallah, M. Al-Riyami *et al.*, "A study of the effects of CO, NO_2, and PM_{10} emissions from the Oman liquefied natural gas (LNG) plant on ambient air quality," *Air Quality, Atmosphere & Health*, vol. 13, no. 10, pp. 1235–1245, 2020.

[41] WHO. (2021). WHO global air quality guidelines: Particulate matter ($PM_{2.5}$ and PM_{10}), ozone, nitrogen dioxide, sulfur dioxide, and carbon

monoxide. *World Health Organization*. [Online]. Available: https://www.who.int/publications/i/item/9789240034228

[42] I. S. Ambrose, S. E. Etuk, O. E. Agbasi *et al.*, "Public health implications of road construction and traffic congestion in a hydrocarbon-polluted environment: An assessment of air and noise pollution," *Revue Internationale de Géomatique*, vol. 34, pp. 335–350, 2025.

[43] C. Nwankwo and D. Ogagarue, "Effects of gas flaring on surface and ground waters in Delta State Nigeria," *Journal of Geology and Mining Research*, vol. 3, no. 5, pp. 131–136, 2011.

[44] I. Manisalidis, E. Stavropoulou, A. Stavropoulos *et al.*, "Environmental and health impacts of air pollution: A review," *Frontiers in Public Health*, vol. 8, 14, 2020.

[45] A. Ite and U. Ibok, "Gas flaring and venting associated with petroleum exploration and production in the Nigeria's Niger Delta," *American Journal of Environmental Protection*, vol. 1, no. 4, pp. 70–77, 2013

[46] J. K. Nduka and O. E. Orisakwe, "Water-quality issues in the Niger Delta of Nigeria: A look at heavy metal levels and some physicochemical properties," *Environmental Science and Pollution Research*, vol. 18, pp. 237–246, 2010.